NAVAL SHIP RESEARCH AND DEVELOPMENT CENTER

Washington, D.C. 20007

NAVAL SHIP RESEARCH AND DEVELOPMENT LABORATORY
Annapolis, Maryland 21402

INVESTIGATION OF THERMOELECTRIC PROPERTIES OF LIQUID METALS

MACHINERY LABORATORY

RESEARCH AND DEVELOPMENT REPORT

November 1969

Report 3058

Report 3058

Investigation of Thermoelectric Properties of Liquid Metals

INVESTIGATION OF THERMOELECTRIC PROPERTIES OF LIQUID METALS

By
Hugh Grant Anderson, Jr.

November 1969 MACHLAB 254 Report 3058

INVESTIGATION OF THERMOELECTRIC PROPERTIES OF LIQUID METALS

A Thesis
Presented to
the Graduate Council of
The University of Tennessee

In Partial Fulfillment
of the Requirements for the Degree
Master of Science

by
Hugh Grant Anderson, Jr.
June 1969

ACKNOWLEDGMENTS

The research reported in this thesis is part of a general investigation on physical properties of electrically conducting fluids. The author gratefully acknowledges the support from the UT/NASA Sustaining University Program NASA grant No. 43-001-021, sub-account No. 141370-3154R.

The research reported herein was proposed and directed by Dr. R.G. Bressler.

The actual measurements for this thesis were performed at the U.S. Naval Ship Research and Development Center; Annapolis Division; Annapolis, Maryland. The author is grateful for use of the Center's instrumentation facilities and the kind support which permitted graduate studies and the carrying out of this work. For this purpose the author expresses thanks especially to Mr. A. B. Neild and many of his associates in the Power and Propulsion Division. Recognition also goes to those who assisted in the preparation of drawings and typing of the thesis.

ABSTRACT

An apparatus has been designed and developed for measuring Seebeck potentials and electrical resistivities of corrosive liquids up to temperatures of about 600°C. A complete description of the test apparatus and the procedures used in its initial operation up to 600°C are given. Experimental results for the absolute Seebeck coefficients of sodium and potassium are in good agreement with published values from previous investigations performed at temperatures up to 400°C. The obtained values are in the range of 0-40 uV/°C, potassium having the highest values. These results indicate that the absolute Seebeck coefficients in the liquid state seem to be higher than that of the solid state by as much as a factor of about three for both metals. Quantitative calculations indicate that these particular metals offer more advantages thermoelectrically in the liquid state than in the solid state. Results for the electrical resistivity were too high by about four orders of magnitude and therefore they were considered to be erroneous.

It is proposed how to improve the test apparatus to obtain more meaningful resistivity values and how to extend the temperature range of the facility to the design temperature 800°C. It is suggested that the thermoelectric properties of liquid semiconductors be investigated in the future.

TABLE OF CONTENTS

LIST OF TABLES

LIST OF FIGURES

CHAPTER I

INTRODUCTION

A study of the state of the art on liquid metals reveals that there is little information on thermoelectric properties available. Four previous investigations[1-4*] which were aimed to determine the absolute Seebeck coefficients of alkali metals covered a range of temperatures up to 400°C. Ten polyvalent metals[4, 5] have been investigated up to 750°C.

The compatibility of a liquid and its container limits the extent to which the absolute Seebeck coefficient of the liquid can be investigated with respect to temperature. Thus, Jackson[6] indicates that most glasses and ceramics are seriously corroded by alkali metal beyond 300°C. Prior investigators[1-4] report the use of such materials in determining the Seebeck coefficients for alkali metals. Although metals are suited for containing liquids during electrical resistivity and thermal conductivity measurements, attempts to use metal containers for Seebeck voltage measurements have been unsuccessful.[7] This may explain why, in the case of alkali metals, far more information with regard to the thermal conductivity and electrical resistivity is available than for the Seebeck coefficient.

*Superscript numbers refer to correspondingly numbered references on page 40.

Therefore the present investigation was undertaken and an experimental apparatus was designed for determining Seebeck potentials and the electrical resistivities of alkali and other metals up to temperatures of 800°C. A description of the experimental apparatus and the procedures used in its operation is given in this thesis. Results and an estimation of their accuracy for determining the absolute Seebeck coefficient of liquid sodium and potassium up to about 600°C and mercury up to 200°C are presented and compared with existing data. Recommendations are presented for improving certain features of the apparatus such that the intended design objective may eventually be attained.

CHAPTER II

THEORY

In this chapter, the theory of the transport properties relating to thermoelectricity is discussed in two parts. The first part consists of a summary of the historical development of the theory for solid-state metals. This is followed by a similar discussion of the theory on liquid-state metals.

1. SOLID-STATE MATERIALS

The Seebeck, Peltier, Thomson, Fourier, and Joule effects discovered in the nineteenth century and described in a number of texts play an important role in the study of thermoelectric phenomena.

The first mathematical expressions for the transport properties relating to thermoelectricity were in the development stages in 1804 when Biot proposed an expression for the propagation of thermal energy through a solid. This gave rise to Fourier's equation of heat conduction in 1822.[9]

In 1900, the major advances that were to place the theory of transport properties on a solid foundation had already been made. Such advances were the formulation of Ohm's Law (1826),[10] the Joule Heating Effect (1842),[10] and the Wiedmann-Franz Ratio (1853).[11]

This was followed by the discovery of the relationship between the Seebeck (1821) and the Peltier (1834) effects when Thomson discovered the Thomson effect in 1856.[12]

In 1900, the real substance of the transport theory began when Drude[12] recognized free electrons in solids and developed his Kinetic Model of Collision between free electrons and a stationary atomic lattice. By treating electrons as a gas moving through and colliding with the atomic lattice, Drude was able to derive an expression for the electrical conductivity and the thermal conductivity given by (1) and (2)*

$$\sigma = \frac{n q^2}{m} \tau \tag{1}$$

$$k = 3 \frac{K^2 n T}{m} \tau \ . \tag{2}$$

This led to the Wiedemann-Franz-Lorenz law:

$$\frac{k}{\sigma} = 3 \left(\frac{K}{q}\right)^2 T = L_o T \tag{3}$$

In 1905, H. A. Lorentz derived the equations for the transport properties by applying Boltzmann's transport equation to the Drude model. The Lorentz solution sufficed to account for all thermal, electric, and magnetic effects.[12]

Partial results of the simplified Lorentz solution are presented by Soo[12] in the following form:

For a metal whose free electrons obey Fermi-Dirac distribution law, the Seebeck, Peltier, and Thomson coefficients become

*A list of all symbols used is given at the end of this thesis

$$S = 1/2\frac{\pi^2 K^2 T}{q\epsilon_o} \tag{4}$$

$$\Pi = 1/2\frac{\pi K^2 T^2}{q\epsilon_o} \tag{5}$$

$$\gamma = 1/2\,\frac{T}{q}\frac{\pi^2 K^2}{\epsilon_o}\,. \tag{6}$$

In general, the main difficulties in theoretical calculations for transport properties lie in predicting the relaxation time and the distribution of charge carriers. Although these difficulties have been overcome to some extent for solid-state materials by application of quantum statistics, the difficulties still exist for liquid-state materials which will be discussed in the following paragraphs.

2. LIQUID-STATE METALS

Ziman[13] has recently used the theory of pseudopotentials (Phillips and Kleinmann)[14] to formulate expressions for the electrical resistivity and the absolute Seebeck coefficient of liquid metals. Prior theories as mentioned by Cusack[15] have been proved inadequate for the liquid state, the reason being that liquids posess disordered structures, whereas the earlier theories were based on solid-state physics which is suitable only for ordered structures.

A number of investigators has made theoretical calculations for the electrical resistivity of a variety of liquid metals, Ziman[13] and Bradley, Faber, Wilson, and Ziman.[15] According to Harrison[16] their results were consistently

overestimated by a factor of the order of three. Harrison reported that he was unable to obtain any meaningful values for the alkali metals. However, Sundstrom[17] carried out calculations for the electrical resistivity and the absolute Seebeck coefficient and reported that the results were in fair agreement with experimental values. Marwaha and Cusack[18] made additional calculations for the absolute Seebeck coefficient but could not come up with any meaningful results. The wide variation of theoretical results among the above investigations may be attributed to the fact that Ziman's equations require a knowledge of structure factors of the liquid metals in question. This information is obtained normally from X-ray diffraction data.

Cusack and Marwaha[18] concluded that theoretical calculations cannot be compared with experimental values until more reliable knowledge on liquid metal structure is available. Harrison has reached the same conclusion, emphasizing the fact that the structure factors in a liquid represent an unsolved theoretical problem.[16]

CHAPTER III

METHOD OF EXPERIMENT

The experimental equipment and methods used in this investigation are presented in this chapter.

1. LIQUID-METAL TEST APPARATUS

Figure 1 is a schematic of the liquid-metal test apparatus. Design details are given in Appendix A. In this apparatus the liquid metal is contained within a beryllia tube* (1" long x 1/4" ID x 1/2" OD) located inside a metal container.

The metal parts directly in contact with the liquid metal are made of tantalum. These parts are designated in Figure 1 by "upper tantalum part" and "lower tantalum part." The upper tantalum part is designed to permit filling the apparatus through a removable tantalum plug and to permit the necessary thermal expansion of the liquid. Leakage at the top of the beryllia tube is prevented by means of a beryllia to tantalum face seal. The lower tantalum part prevents leakage from the bottom by means of a similar seal.

The remaining part of the test container is made of stainless steel and is designated as "cap" in Figure 1. The cap provides a means for keeping the beryllia tube under compression. This is accomplished by initially tightening

*American Lava Corporation, Chattanooga, Tennessee.

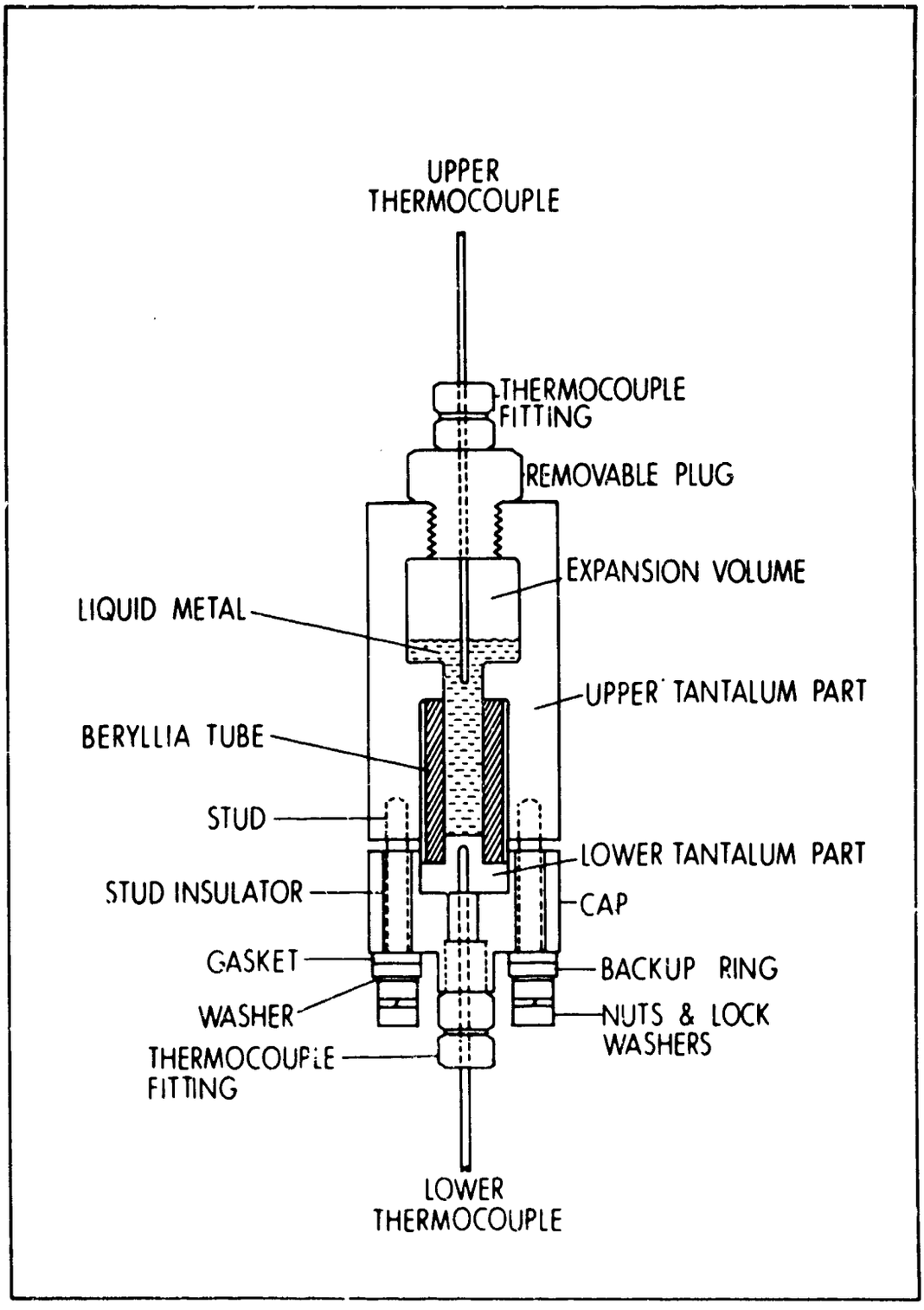

FIGURE 1
LIQUID METAL TEST APPARATUS

the nuts (on the studs indicated in Figure 1 extending from the upper tantalum part) against the cap. Upon heating of the container, compression of the beryllia cube is attained by taking advantage of the thermal expansion of the beryllia, tantalum, and stainless steel parts.

To avoid calibrating for the resistivity and Seebeck potentials of the various metal parts of the container, the upper tantalum part is electrically insulated from the lower parts. Mullite* tubes electrically insulate the studs from the cap. A Garlock** gasket insulates the nuts and washers from the exposed face (bottom) of the cap. A metal backup ring is used to prevent damage to the gasket upon tightening the nuts.

Electrical contacts with the liquid were made through 1/16" OD tantalum sheathed chromel alumel thermocouples with grounded junctions. The thermocouples were manufactured by the Thermo Electric Company.*** They were secured within the removable plug and the cap by means of standard thermocouple fittings.*** Alumel current probes were attached to the tantalum thermocouple sheaths for resistivity measurements. A distance of 1-1/16" was maintained between the thermocouple junctions. Prior to filling with liquid metal, a rod of 1.000" length was placed in the apparatus. The upper thermocouple sheath was then lowered until the tip contacted the rod. The thermocouple fitting was then tightened around the sheath. Figure 2 is a schematic of the upper and lower thermocouple junction assemblies.

*Coor's Porcelain Co.; Golden, Colorado.
**Garlock Corp., Inc. (tradename).
***Thermo Electric Company, Saddle Brook, New Jersey.

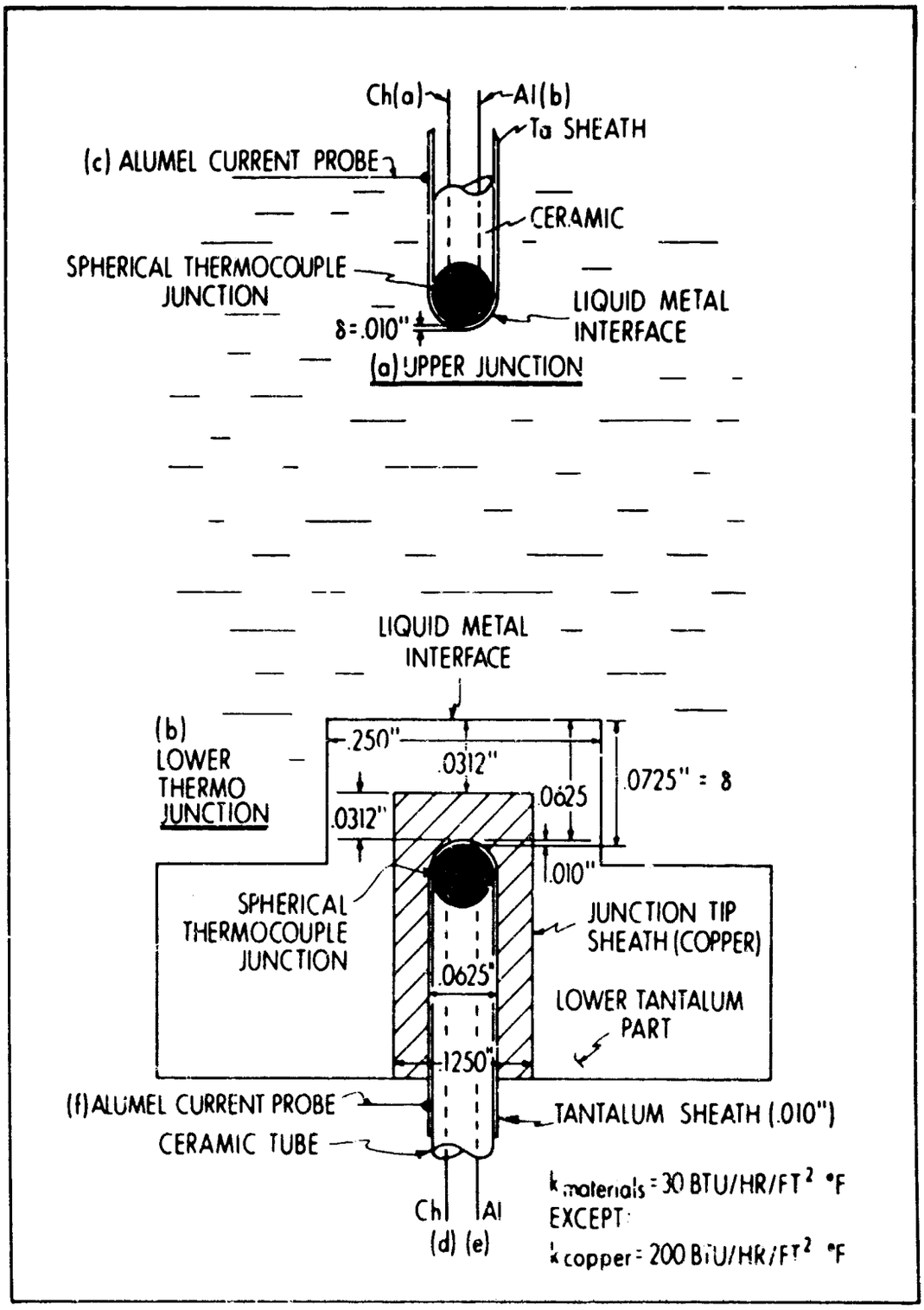

FIGURE 2
THERMOCOUPLE JUNCTION ASSEMBLIES

2. FILLING OF THE TEST APPARATUS

The apparatus described in Part I was filled with the liquid-metal sample* in the presence of an argon atmosphere, to avoid contamination and reactions by coming in contact with air upon heating. For this purpose a Labconco glove box was used. (No inert gas was used in the case of mercury.) The argon was 99.99 per cent pure. A $CaSO_4$ filter was placed in the argon supply line to remove extraneous sources of moisture. Sodium and potassium both were melted in a thoroughly cleaned stainless steel beaker on a hot plate. While the sodium was transferred to the apparatus by means of a small syringe, the potassium was poured directly into the beryllia tube. The mentioned beaker was cleaned with a detergent, degreased with trichloroethylene, flushed with acetone, and dried with argon. The mineral oil which was used by the supplier to seal Na and K in their shiping containers was removed by rinsing the Na and K samples several times with trichloroethylene and drying the same with argon prior to placing in a preheated clean beaker for melting.

Once the container was filled, the removable plug was installed. The apparatus was then allowed to cool before it was transferred from the glove box to the ceramic container shown in Figure 3.

*Samples purchased from City Chemical Corporation, New York, New York.

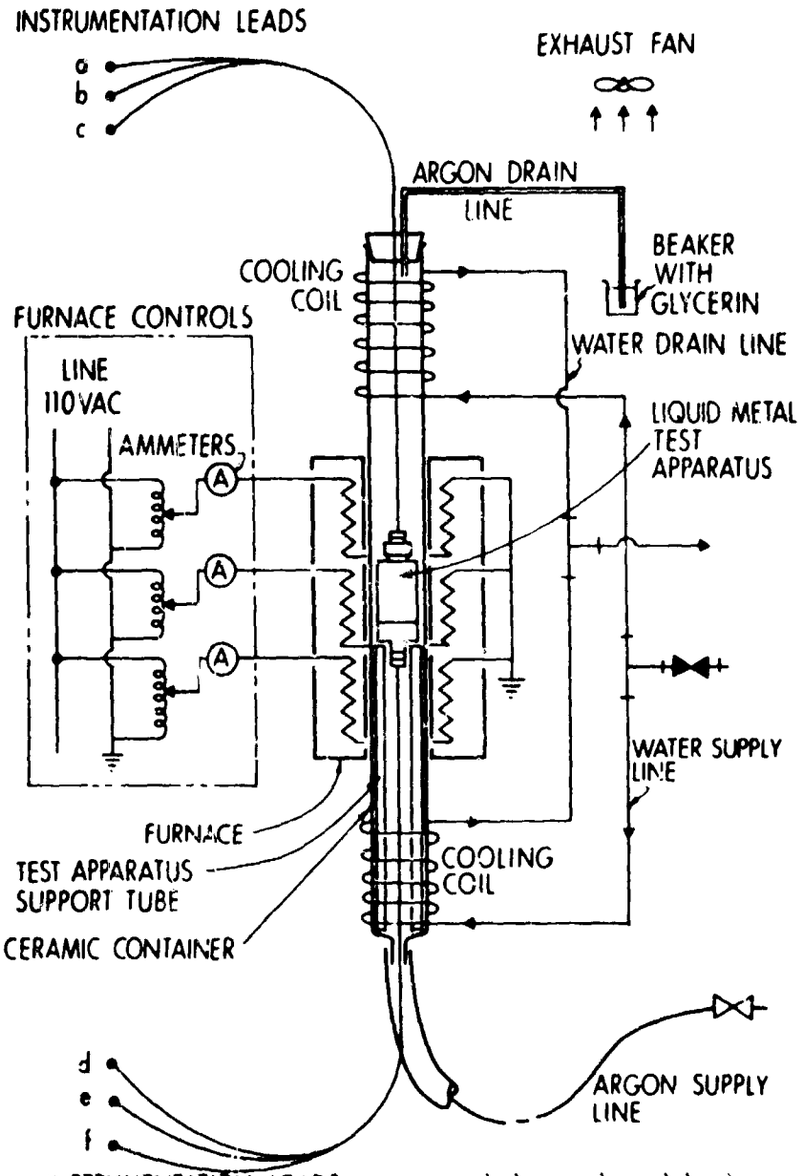

INSTRUMENTATION LEADS: wires a and d are chromel leads from the upper and lower thermocouples. Wires b and e represent the alumel leads from the same thermocouples. Wires c and f are the current probes which are attached to the tantalum sheaths of the thermocouples.

FIGURE 3
CERAMIC CONTAINER

3. CERAMIC CONTAINER

The ceramic container (a 24-in. long tube) was used to keep the test aparatus under an argon atmosphere while heated electrically within the furnace.

The arrangement is illustrated in Figure 3 and pictured in Figure 4. The test apparatus was supported within the ceramic container by a smaller ceramic tube. Argon entered at the bottom of the container and left at the top where the gas bubbles could be observed when they were passing through a beaker which was filled with glycerin. An exhaust fan pulled the argon out of the laboratory room.

The cooling coils, indicated at the top and bottom of the ceramic container in Figure 3, were installed in order to reduce the temperature at both ends of the container.

4. FURNACE AND CONTROLS

The furnace indicated in Figure 3 and pictured in Figure 4 is a Satec Model SF furnace. It contains three separate heating zones. Each zone is rated at 7.5 amperes and 110 volts. The controls were three 7.5 ampere powerstats; their currents were read at three ammeters placed in the circuits.

5. METHOD OF MEASUREMENT

All measurements were obtained under unsteady state conditions over a temperature range from 25°C to 600°C. A complete heating period for a test run took approximately two hours.

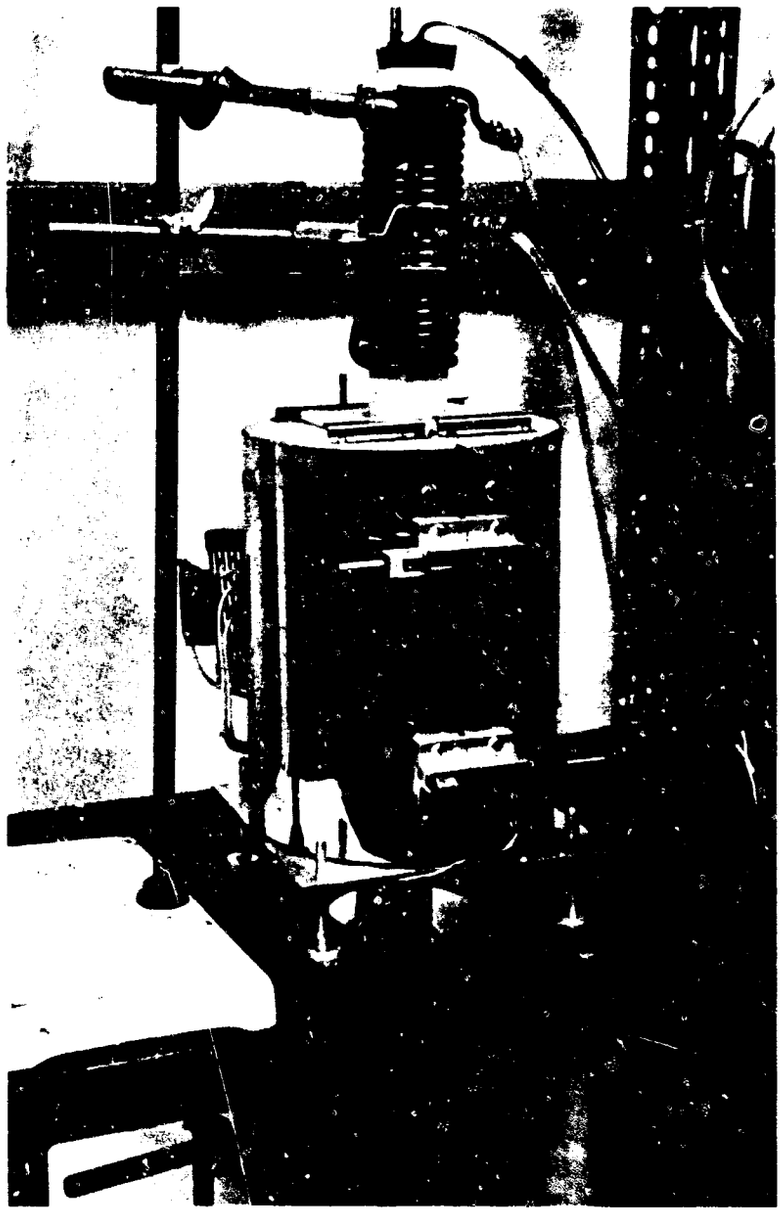

FIGURE 4
FURNACE AND CERAMIC CONTAINER

Seebeck coefficient. The method of obtaining the Seebeck coefficients was based on the measurement of the Seebeck emfs between the liquid samples and a counter electrode (either chromel or alumel) at different mean temperatures. The schematic arrangement of the measuring circuit is shown in Figure 5. The temperature differences ($T_H - T_C$) ranged from 5°C to 30°C in the experiments.

For zero electric current flow*, the Seebeck coefficient, S, is defined as

$$S_{SW} = \lim_{\Delta T \to 0} \frac{V_{SW}}{\Delta T} = \frac{dV_{SW}}{dT} \tag{7}$$

where S_{SW} is the Seebeck coefficient as measured between materials S and W, ΔV_{SW} is the voltage between the same materials and

$$\Delta T = T_H - T_C$$

is the difference between the hot and cold temperatures. Therefore the voltage V_{SW} is given by

$$V_{SW} = - \int S_{SW}\, dT . \tag{9}$$

As shown in Figure 5 potentials V_{SCh} and V_{SAl} were measured between two identical thermocouple wires and the samples.

Writing V_{SCh} and V_{SAl} in the form of Equation (9), then

$$V_{SCh} = - \int_{T_O}^{T_C} S_{Ch}\, dT - \int_{T_C}^{T_H} S_S\, dT - \int_{T_H}^{T_O} S_{Ch}\, dT \tag{10}$$

*Open circuit condition in Figure 5.

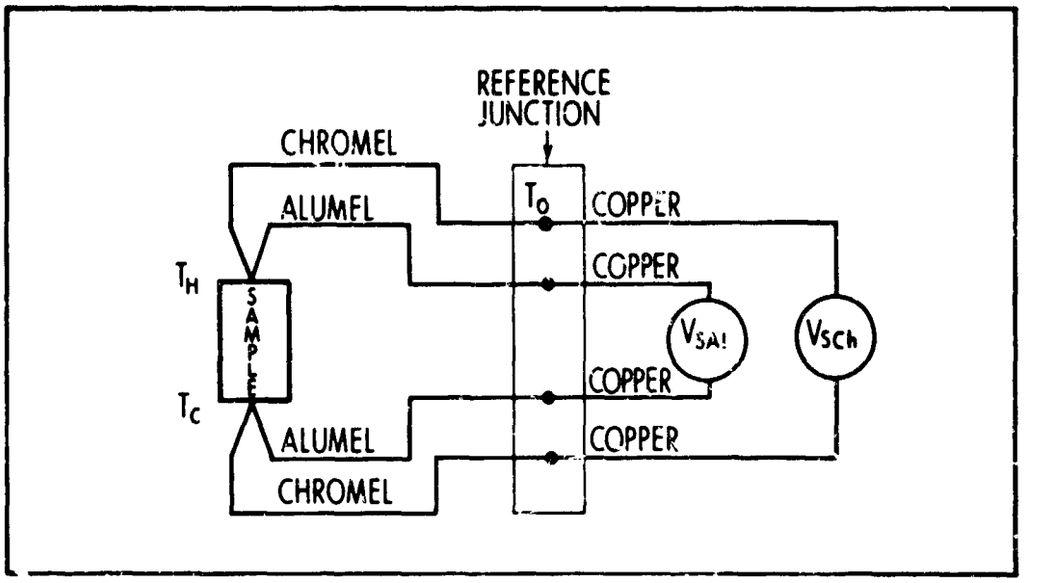

(a) Circuit for measuring Seebeck Voltages
Open Circuit Condition ≡ Zero Current Flow
See Figure 5-b

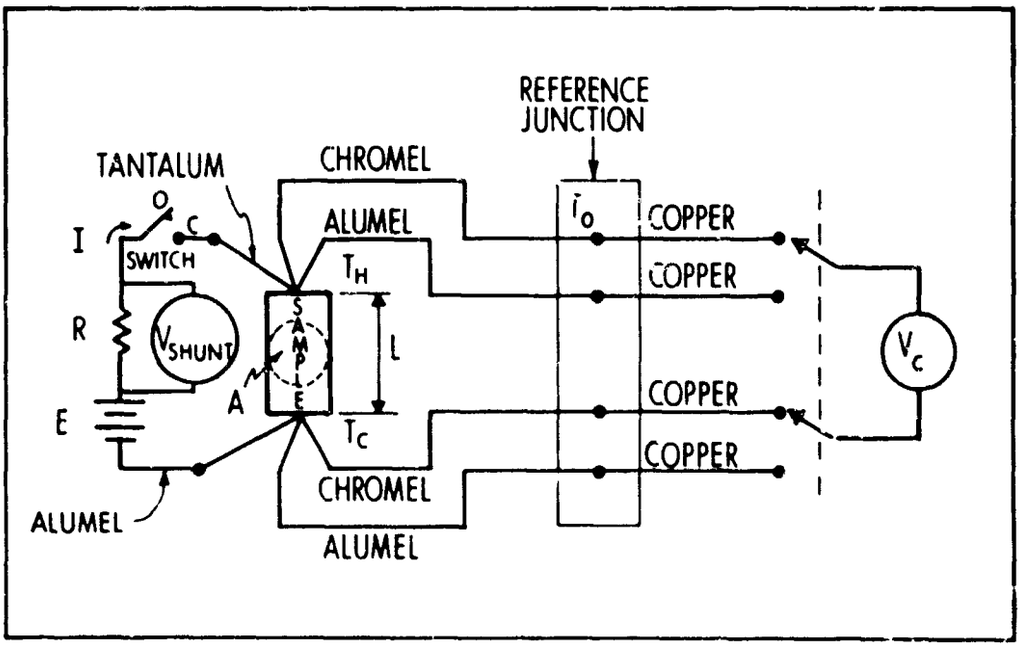

(b) Circuit for resistivity measurements
Position of Switch: O: Open Circuit;
C: Closed Circuit

FIGURE 5
MEASURING CIRCUITS

and

$$V_{SAl} = -\int_{T_O}^{T_C} S_{Al}\, dT - \int_{T_C}^{T_H} S_S\, dT - \int_{T_H}^{T_O} S_{Al}\, dT \qquad (11)$$

where S_{Ch}, S_{Al}, and S_S are the absolute Seebeck coefficients for chromel, alumel, and the liquid-metal sample, respectively.

Equations (10) and (11) can be rewritten as

$$V_{SCh} = \int_{T_C}^{T_H} S_{Ch}\, dT - \int_{T_C}^{T_H} S_S\, dT = \int_{T_C}^{T_H} (S_{Ch} - S_S)\, dT. \qquad (12)$$

and

$$V_{SAl} = \int_{T_C}^{T_H} (S_{SAl} - S_S)\, dT. \qquad (13)$$

It is obvious that if $(T_H - T_C)$ were small, S_{Ch}, S_{Al}, and S_S can be treated as if they were independent of temperature over the region of integration in Equations (12) and (13). Hence we write

$$V_{SCh} = (S_{Ch} - S_S)(T_H - T_C) \qquad (14)$$

and

$$V_{SAl} = (S_{Al} - S_S)(T_H - T_C). \qquad (15)$$

From Equations (14) and (15) we may calculate the Seebeck coefficient of the sample, S_S, by either of the following two equations

$$S_S = S_{Ch} - \frac{V_{SCh}}{T_H - T_C} \tag{16}$$

or

$$S_S = S_{Al} - \frac{V_{SAl}}{T_H - T_C} \tag{17}$$

where S_{Ch} and S_{Al} are known physical properties, while V_{SCh}, V_{SAl}, and $T_H - T_C$ are measured. In Figure 6 the absolute Seebeck coefficients of chromel (S_{Ch}), alumel (S_{Al}), and platinum (S_{Pt}), which have been used for the evaluation of the measurements, are shown.

Electrical resistivity. Figure 5 illustrates how the thermocouples had been used as voltage probes. The resistivity of the sample was determined from the equation,

$$\frac{1}{\sigma} = \frac{A}{L}\left[\frac{V_C - V_{SW}}{I}\right] \tag{18}$$

where A is the area of the sample perpendicular to the direction of current flow, I. L is the distance between both thermocouple probes. With the switch shown in Figures 5 and 7 in its closed position, the potential voltage E caused a current I through the resistance R and thus through the sample, since these two resistances were in series. When the current was flowing, the voltage drop V_C was measured. Throughout the test runs a small temperature difference

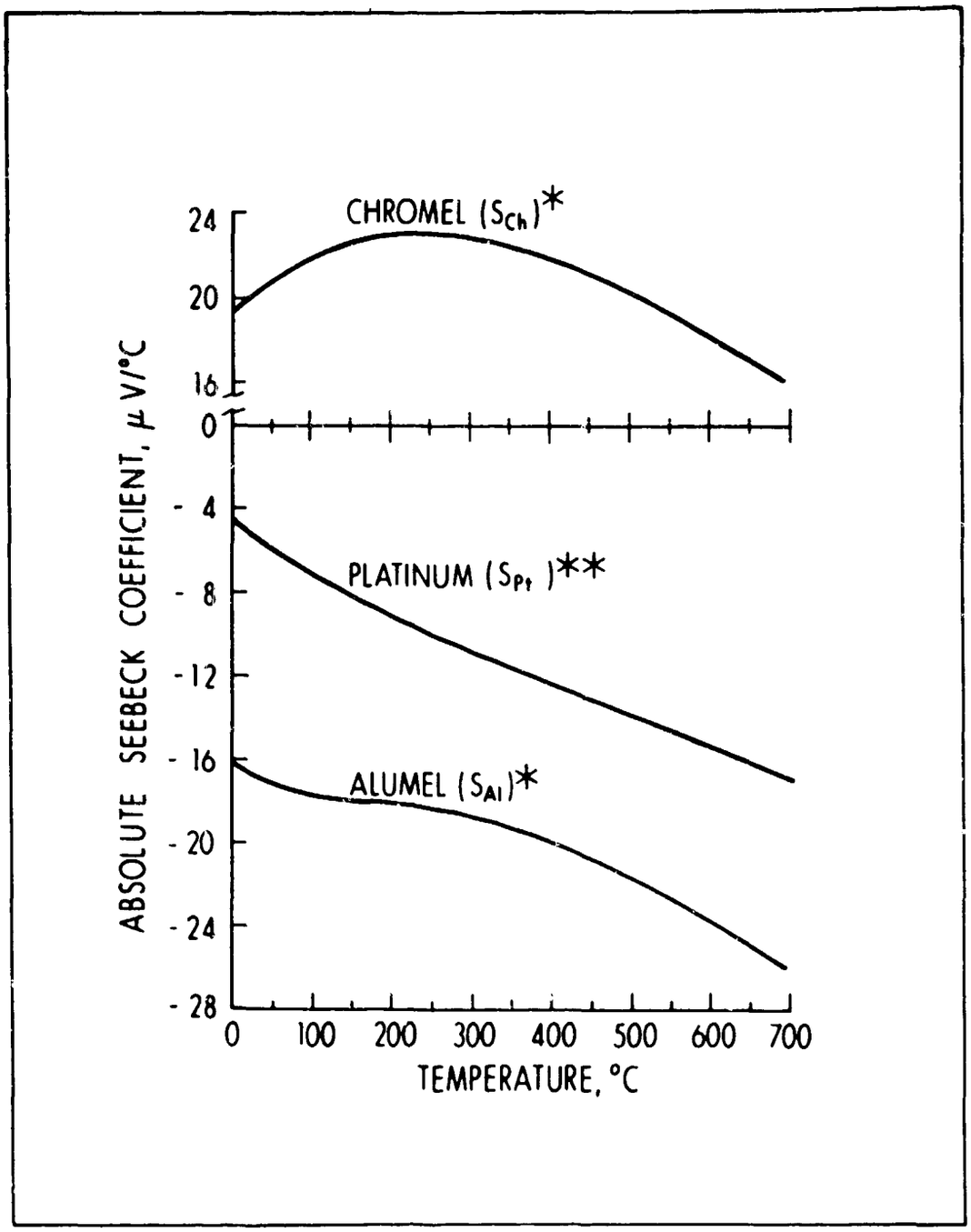

FIGURE 6
ABSOLUTE SEEBECK COEFFICIENT FOR CHROMEL, ALUMEL, AND PLATINUM

*Source: White, R. M., Sandia Laboratory Report SC-RR-68-588, 1968.
**Source: Landolt-Bornstein, "Physikalisch-chemische Tabellen," 6th ed. Vol. 11/6, Springer, Berlin, 1959, p. 929/31.

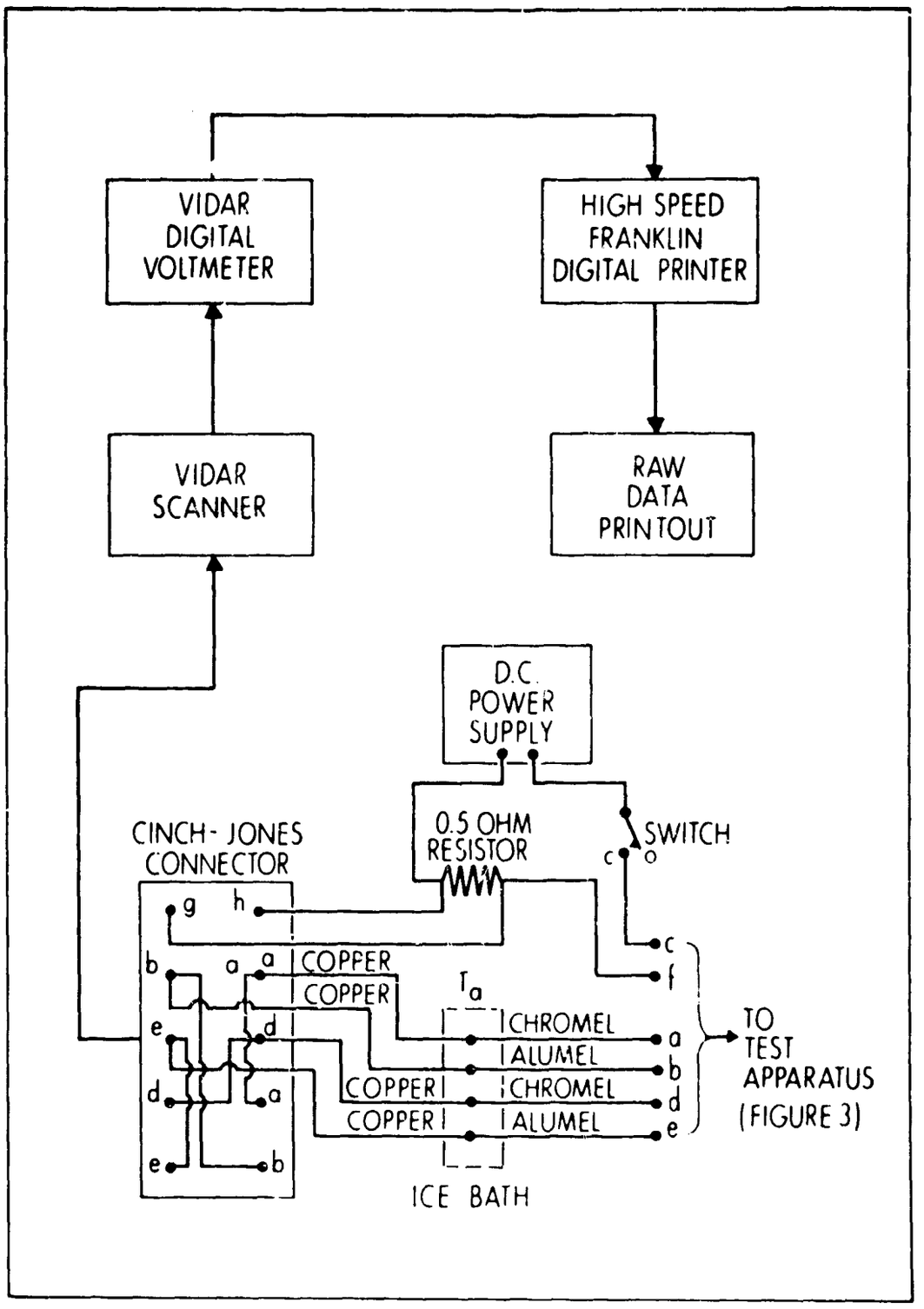

FIGURE 7
INSTRUMENTATION SCHEMATIC

$T_H - T_C$ existed between both ends of the sample. The voltage difference across the liquid sample due to the current flow had been determined by subtracting the Seebeck voltage V_{SW} as described before in Equation (9) from the combined voltage V_C which is given by

$$V_C = IR_S + V_{SW} \quad (19)$$

6. INSTRUMENTATION

The thermocouple leads and current probes which were indicated in Figures 2 and 3 as instrumentation leads, corresponded to those illustrated in Figure 7. The purpose of the scanner which also is shown in Figure 7 was to scan the voltage terminals on the Cinch-Jones connectors (a-b, d-e, a-d, b-e, and g-h) and to relay a signal to the digital voltmeter so that the voltage at each set of terminals could be measured. The digital voltmeter in turn signaled the printer to print the measured values. The ice bath provided a reference voltage for temperature measurements. The parameters measured across the terminals are listed below in the order that they were obtained.

Open Circuit Condition

Terminal	Parameter Measured
a-b	Temperature at upper junction
d-e	Temperature at lower junction
a-d	Seebeck voltage of sample relative to chromel
b-e	Seebeck voltage of sample relative to alumel.

Closed Circuit Condition

Terminal	Parameter Measured
g-h	Voltage drop across 0.5-ohm resistor
a-b	Temperature at upper junction
d-e	Temperature at lower junction
a-d	Combined voltage due to Seebeck voltage of sample relative to chromel and due to IR potential across liquid sample
b-3	Combined voltage due to Seebeck voltage of sample relative to alumel and due to IR potential across liquid sample.

After the closed circuit parameters were measured the open circuit parameters were immediately remeasured to check if the temperatures of the sample had changed in the meantime. Generally, no appreciable change was noted.

A complete listing of the instrumentation used in the experiment is given below:

Instrument	Description
Digital Voltmeter	Vidar 520 Integrating Digital Voltmeter, Model 520-01, Serial 2-231, Assembly 1300-01,
Scanner	Vidar 604 Master Scanner, Mode 604-01, Serial 2-198, Assembly 1900-01,
Printer	Franklin Model 012200-11-6612R, Serial 367-506-100 High Speed Digital Printer,
Glove Box	Labconco Glove Box, Serial 4281.

Figure 8 is a photograph of the instrumentation and equipment used in this investigation.

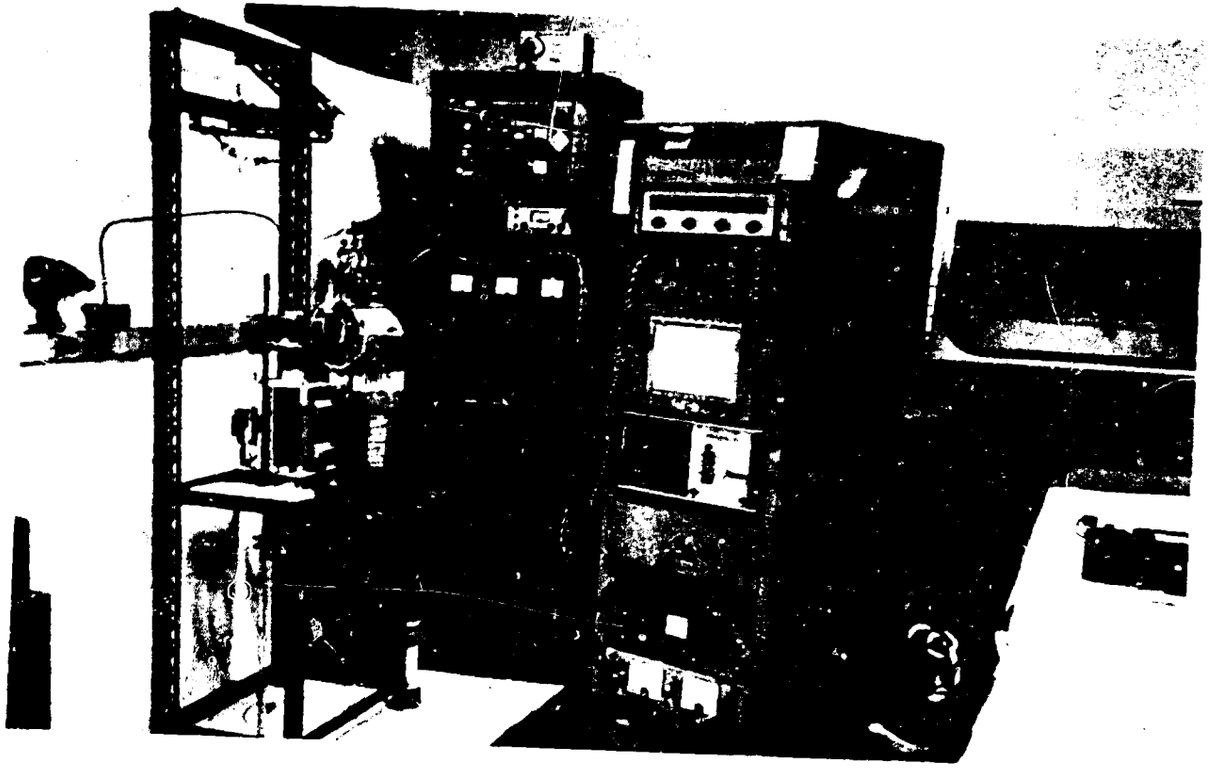

FIGURE 8
TEST EQUIPMENT AND INSTRUMENTATION

7. DATA REDUCTION

Table I illustrates the procedure which was used to reduce the measured data. Column (13) in Table I was obtained from the equations

$$S_{Pt} = -12.48 - 1.59\left(\frac{T-400}{100}\right) + 0.021\left(\frac{T-400}{100}\right)^2 \frac{\mu V}{^\circ C} \qquad (20)$$

for $200^\circ C \leq T \leq 200^\circ C$

$$S_{Pt} = -6.48 - 1.584\left(\frac{T-80}{60}\right) + 0.2114\left(\frac{T-80}{60}\right)^2 \frac{\mu V}{^\circ C} \qquad (21)$$

for $-40^\circ C \leq T \leq 200^\circ C$

which were empirically determined by a least squares fit of the absolute Seebeck coefficient for platinum as given by Reference 20. The other columns are self-expanatory.

TABLE I

EXPERIMENTAL DATA AND DATA REDUCTION SAMPLE*

Measured Experimental Data				Temperature Conversion		Temperature Calculations	
T_H	T_C	$S_{NaCh}\Delta T$	$S_{NaAl}\Delta T$	T_H	T_C	ΔT	$\bar{T}$
(mV)	(mV)	(μV)	(μV)	(°C)	(°C)	(°C)	(°C)
(1)	(2)	(3)	(4)	(5)	(6)	(7) = (5) - (6)	(8) = [(5) + (6)] ÷ 2
16.253	15.345	.803	+105	396.50	375.00	21.50	385.75

Seebeck Coefficient Calculations							
S_{NaCh}	S_{NaAl}	S_{ChPt}†	S_{AlPt}†	S_{Pt}‡	S_{Na}	S_{Na}	$\bar{S}_{Na}$
(μV/°C)	(μV/°C)	(μV/°C)	(μV/°C)	(μV/°C)	(μV/°C)	(μV/°C)	(μV/°C)
(9) = $\frac{(3)}{(7)}$	(10) = $\frac{(4)}{(7)}$	(11)	(12)	(13)	(14) = (9) + (11) + (13)	(15) = (10) + (12) + (13)	(16) = $\frac{[(14) + (15)]}{2}$
-37.35	+4.88	+34.41	-7.64	-12.26	-15.20	-15.02	-15.11

*From Reading 21 of sodium test sample on 11/11/68; heater current = 6 amperes.

†White, R.M., Sandia Laboratory Report SC-RR-68-588, 1968.

‡Landolt-Bornstein, "Physikalisch-chemische Tabellen," 6th ed. Vol. 11/6, Springer, Berlin, 1959, p. 929/31.

CHAPTER IV

RESULTS OF INVESTIGATION

The results for the absolute Seebeck coefficients of sodium, potassium, and mercury are summarized in Tables II, III and IV, respectively. Corresponding graphs of the results along with the results of previous investigations are presented in Figures 9, 10, and 11.

TABLE II

SUMMARY OF SEEBECK COEFFICIENT CALCULATIONS FOR SODIUM

$\bar{T}$ °C	S_{Na}* μV/°C	S_{Na}** μV/°C	$\bar{S}_{Na}$+ μV/°C
220	-12.8	-10.9	-11.9
242	-10.2	-11.1	-10.7
242	-10.2	-11.1	-10.7
286	-12.7	-13.6	-13.1
296	-11.9	-12.3	-12.1
309	-13.6	-15.0	-14.3
320	-14.7	-12.4	-13.5
340	-16.3	-16.2	-16.2
343	-12.8	-13.5	-13.1
348	-14.3	-14.2	-14.2
355	-15.5	-15.7	-15.6
364	-13.4	-13.4	-13.4
386	-15.2	-15.0	-15.1
410	-14.5	-16.2	-15.4
422	-16.4	-16.4	-16.4
439	-16.6	-16.4	-16.5
450	-16.5	-16.4	-16.4
460	-16.6	-16.0	-16.3
470	-16.1	-15.7	-16.4
475	-16.1	-15.4	-15.8
478	-15.6	-15.2	-15.4
492	-15.2	-15.0	-15.1
503	-15.6	-15.2	-15.4
515	-15.6	-15.2	-15.4
524	-15.6	-15 0	-15.3
557	-14.3	-14.4	-14.3
570	-15.1	-14.2	-14.7
575	-15.2	-13.9	-14.5
585	-14.4	-13 4	-13.9
594	-12.3	-12.5	-12.4

*Absolute Seebeck coefficient determined from measurements using the chromel counter electrode.

**Ditto, except using the alumel electrode.

+Average absolute Seebeck Coefficient.

TABLE III

SUMMARY OF SEEBECK COEFFICIENT CALCULATIONS FOR POTASSIUM

$\bar{T}$	S_K*	S_K**	$\bar{S}_K$+
°C	μV/°C	μV/°C	μV/°C
66	-13.4	—	—
95	-16.1	—	—
112	-15.1	—	—
133	-15.4	—	—
154	-15.1	—	—
175	-15.8	—	—
197	-21.0	—	—
243	-22.0	—	—
254	-21.9	—	—
292	-23.6	—	—
311	-22.9	-23.5	-23.2
325	-22.5	-25.5	-24.0
332	-25.4	-24.5	-25.0
341	-24.1	-24.4	-24.1
348	-24.4	-24.3	-24.3
358	-24.9	-24.9	-24.9
368	-24.7	-24.8	-24.8
376	-24.1	-25.0	-24.5
382	-25.3	-24.5	-24.9
393	-24.4	-25.5	-25.0
403	-26.6	-25.3	-25.9
413	-25.3	-25.4	-25.4
441	-25.5	-27.9	-26.7
460	-26.0	-26.4	-26.2
494	-26.0	-27.6	-26.8
530	-28.3	-27.7	-28.0
574	-32.8	-32.8	-32.8
586	-31.8	-31.5	-31.6

* Absolute Seebeck coefficient determined from measurements using the chromel counter electrode.

**Ditto, except using the alumel electrode.

+Average absolute Seebeck coefficient.

TABLE IV

SUMMARY OF SEEBECK COEFFICIENT CALCULATIONS FOR MERCURY

$\bar{T}$	S_{Hg}*	S_{Hg}**	S_{Hg}+
°C	μV/°C	μV/°C	μV/°C
92	-4.4	-0.1	-2.2
104	-5.5	-2.5	-4.0
118	-4.4	-4.9	-4.6
127	-4.9	-6.1	-5.5
137	-5.4	-6.7	-6.0
144	-7.0	-5.4	-6.2
152	-6.9	-5.0	-5.9
160	-7.9	-8.4	-8.2
164	-8.7	-9.5	-9.1
168	-8.0	-9.4	-8.7
173	-7.5	-6.9	-7.2
176	-6.6	-7.3	-7.0
179	-5.1	-5.8	-5.5
181	-5.6	-5.3	-5.5
185	-4.0	-4.8	-4.4
193	-2.8	-3.9	-3.3
193	-3.1	-4.3	-3.7
200	-1.8	-3.0	-2.4

*Absolute Seebeck coefficient determined from measurements using the chromel counter electrode.

**Ditto, except using the alumel electrode.

+Average absolute Seebeck coefficient.

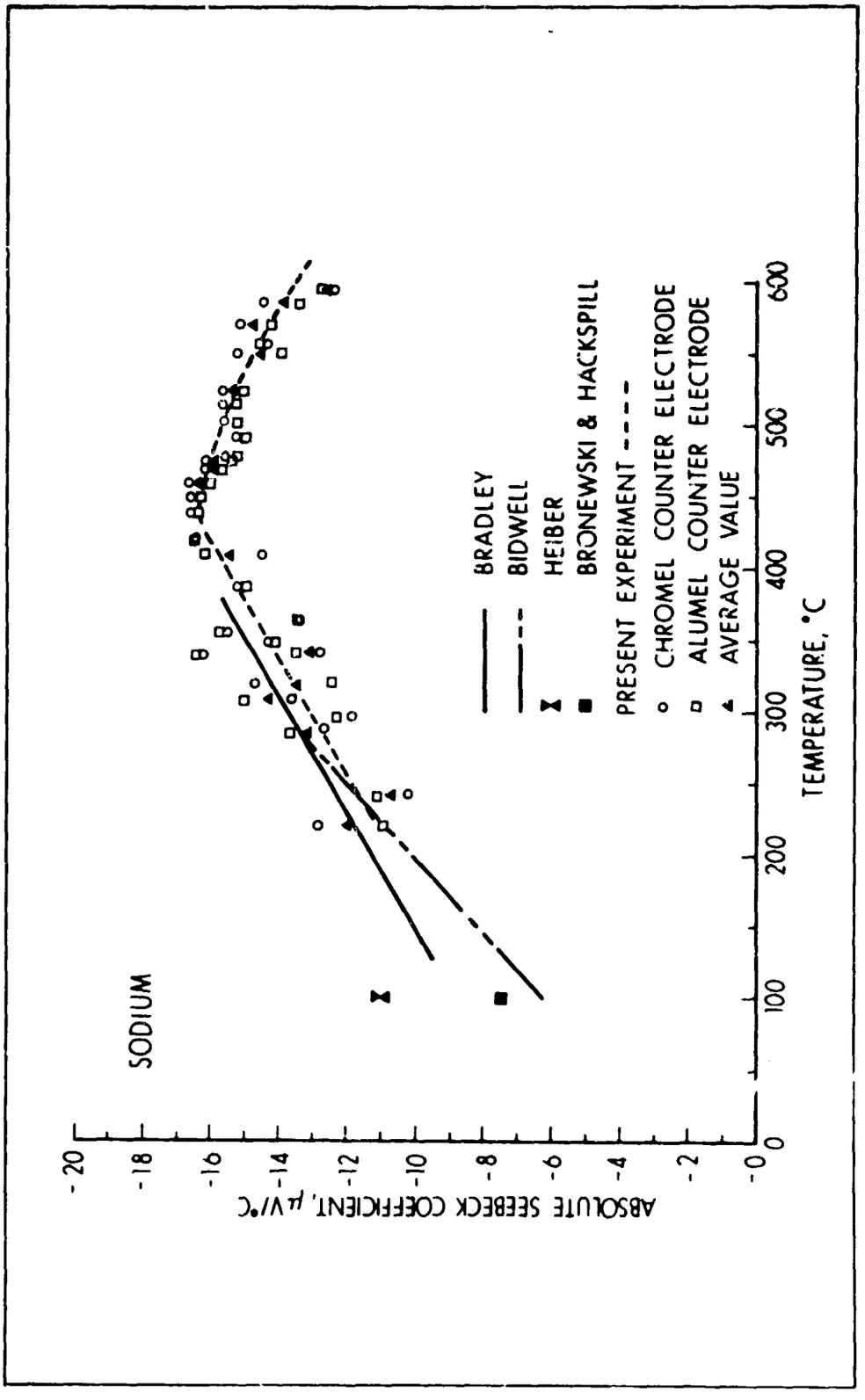

FIGURE 9
ABSOLUTE SEEBECK COEFFICIENT FOR SODIUM

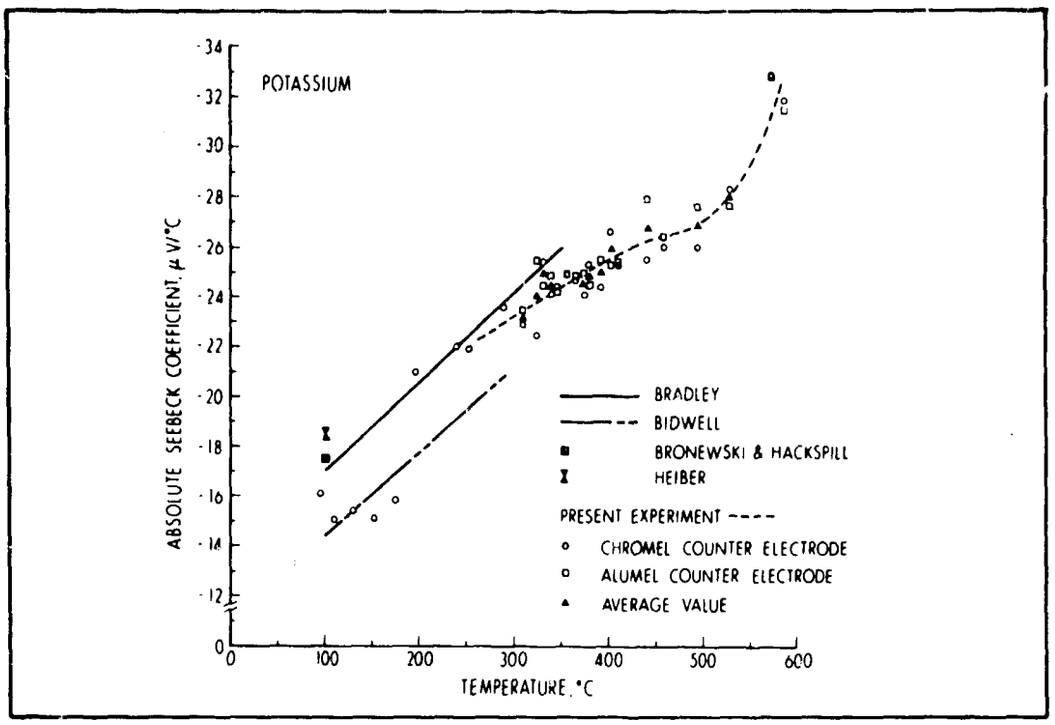

FIGURE 10
ABSOLUTE SEEBECK COEFFICIENT FOR POTASSIUM

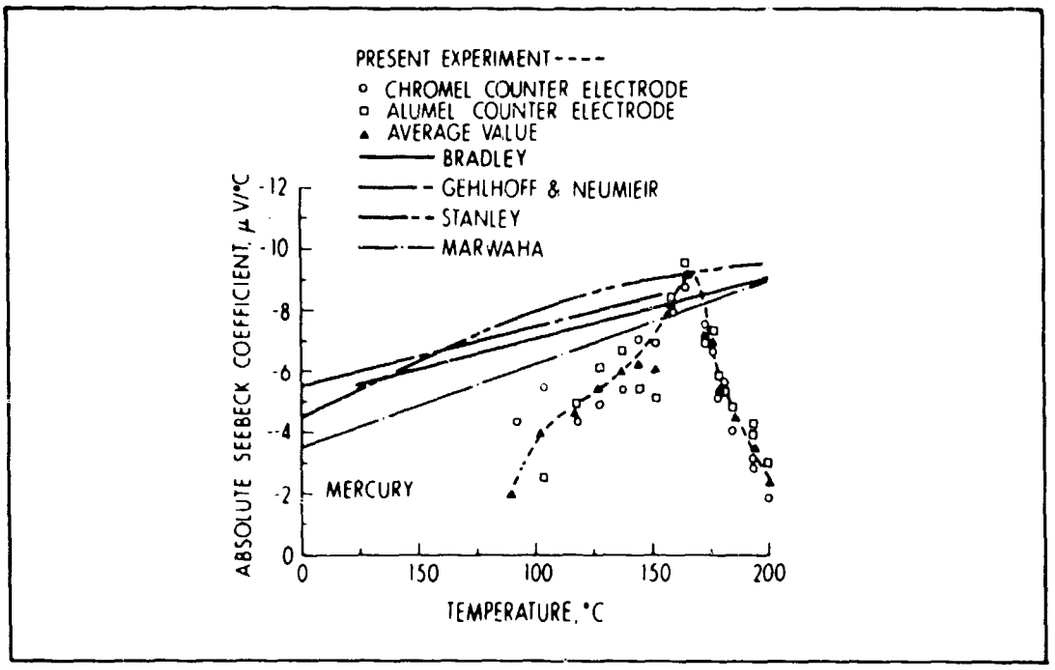

FIGURE 11
ABSOLUTE SEEBECK COEFFICIENT FOR MERCURY

CHAPTER V

DISCUSSION OF RESULTS

In this chapter a discussion of the results for the absolute Seebeck coefficients of sodium, potassium, and mercury is given. An estimate of the errors is given in Appendix B.

1. SODIUM

An examination of Figure 9, p. 30, reveals that the experimental values obtained in the present investigation are not much different from those found by previous investigators. The data points appear to be distributed around a slightly curved line. However, the exact shape of the curve might only be determined with additional data.

One interesting conclusion is that the Seebeck coefficient seems to be much higher in the liquid state. At approximately 450°C the value is about three times greater than that reported at the melting point. Under the assumption that the Wiedemann-Franz-Lorenz law were valid for the liquid state too, the figure of merit Z would be about 17.5 times higher at 450°C than at the melting point at 97°C. This can be shown in the following way:

$$Z = \frac{\sigma S^2}{k} = L_o T S^2 \qquad (22)$$

where T is absolute temperature and

$$\frac{\sigma}{k} = L_o T$$

The ratio of the figure of merits at 450°C and 97°C is then,

$$\frac{(Z)_{T = 450°C}}{(Z)_{T = 97°C}} = \frac{(Z)_{T = 723°K}}{(Z)_{T = 370°K}} = \frac{L_o\ 723°K}{L_o\ 370°K} \cdot \left[\frac{3S_{T=97°C}}{S_{T=97°C}}\right]^2 = 1.95 \left[\frac{3S_{97}}{S_{97}}\right]^2 \simeq 17.5 \tag{23}$$

The ZT product is generally of more interest in thermoelectric generator studies, thus the ZT ratio at 450°C and 97°C is

$$\frac{(ZT)_{T = 450°C}}{(ZT)_{T = 97°C}} \simeq (1.95)\ (17.5) \simeq 35\ . \tag{24}$$

Such increased factors in the liquid state as opposed to the solid state appear to deserve further work.

POTASSIUM

The relative trend in Figure 10, p. 31, of the experimental values obtained in the present investigation appear to be in fair agreement with Bidwell's and Bradley's results. Similar qualitative calculations as given for sodium would indicate an increased ZT product in the case of potassium at say 600°C as compared to 100°C by a factor of about 36 or more.

It will be noted in Table III, p. 28, that some spaces are left blank. As these data were determined from measurements of the Seebeck potentials of potassium relative to alumel, the Seebeck voltages generated by the two metals was about as

small as the magnitude of the errors in the instrumentation. This seems to indicate that in the temperature range of values depicted from Table III, the absolute Seebeck coefficient of potassium is very close to that of alumel. A comparison of the Figure 10 with the graph of the absolute Seebeck coefficient of alumel in Figure 6, p. 19, for the temperature range in question indicate that this relation holds true.

3. MERCURY

The results obtained for mercury seem to be questionable. One reason seems to be the fact that the available chromel-alumel thermocouples are not too accurate in the range of temperature over which the experimental data were obtained. The error in the temperatures measurement for example was given by the manufacturer to be ±4°F (2.2°C) which amounts to 25 - 50 per cent of the order of magnitude of the temperature difference across the sample. Such uncertainty in the temperature difference might lead to Seebeck errors about the same order of magnitude. For this reason the results for sodium and potassium may be questionable below 200°C.

CHAPTER VI

CONCLUSIONS AND RECOMMENDATIONS

In general, it can be concluded that the design of the liquid-metal test apparatus was basically sound and it can be used to measure Seebeck potentials of other liquids, too. It can further be concluded that there was good agreement between the present experimental results and those of prior investigations, as far as the Seebeck coefficients of potassium and sodium are concerned.

1. TEST APPARATUS AND PROCEDURES

Filling the test apparatus was probably the most difficult portion of the experiments. While mercury is liquid at room temperature, sodium and potassium had to be melted before being transferred into the test apparatus. Potassium and particularly sodium had a tendency to solidify immediately upon contact with the unheated test apparatus. This made it difficult to get a large enough metal sample into the apparatus and yet install the upper thermocouple.

Two attempts to test lithium were unsuccessful mainly because the melting point of lithium is too high to be safely handled inside the selected glove box. Therefore, it was attempted to pack the metal into the test apparatus in small chunks. However, it was discovered each time upon subsequent melting during the following tests that there was not enough metal present to bridge the distance between the two thermocouple junctions.

From the preceding discussion on filling, one can conclude that if a material with a high melting point is to be tested in the apparatus described in this investigation a more suitable method of filling is needed. Therefore, it is recommended that the filling process should be accomplished by evacuating the test apparatus and by subsequently using the vacuum to pull in the liquid metal sample.

The electrical resistivity measurements gave results which were several orders of magnitude (about 10^4) too high. Whereas published values of the resistivity of liquid metals fall within the range of micro-ohm centimeters, the actually measured values were as high as tenths of ohm-centimeters. While the reasons are not yet known, it can be thought that such erroneous values might be caused by contact resistances, especially in view of the multiple contact surfaces at the lower thermocouple junction (Compare Figure 2, p. 10). In addition, oxidation films and wetting effects may have had some influence on the resistivity results. As far as the contact resistances are concerned it is proposed that tantalum-tungsten thermocouples be put directly into contact with the liquid metals in the future. For this purpose it is recommended to use tantalum sheathed tantalum-tungsten thermocouples with exposed junction tips. The lower tantalum part (Figure 1, p. 8) would require a hole drilled completely through it, so that upon filling the apparatus, the liquid metals would come in direct contact with the junction formed by the tantalum and tungsten thermocouples wires. The hole diameter should be just large enough to fit the thermocouple sheath in order to prevent a leakage of the liquid metals through the hole. The thermocouples might be installed at the same points as depicted in Figure 1.

Another factor which might have contributed to the high resistivity results is the possibility that void spaces existed in the liquid column. Such a condition would give rise to an effective sample cross sectional area different from the area used in the calculations.

It was mentioned briefly in Chapter I that the high temperatures in this investigation were restricted to 600°C. This restriction was brought about by an improper length of the available thermocouples immersion sheaths. The thermocouple extension leads entered the immersion sheaths via a small transition tube packed with low temperature epoxy. Since the transition tube was located within the ceramic container, the epoxy in the transition tube tended to expand and break the thermocouple wires upon heating the ceramic container. To avoid such occurrences a cooling coil was placed around each end of the ceramic container in order to remove heat from the vicinity of the transition tubes. The cooling coil did not have enough cooling capacity to surpass a temperature of about 600°C. That is why the test apparatus was heated up to 600°C only.

On the other hand, if the immersion sheaths had been long enough to extend to the outside of the ceramic container, the tests could probably have been made as high as 800°C, and the cooling coils would have been unnecessary. Therefore, it is recommended that for the test set up as illustrated by Figure 3, p. 37, the thermocouple immersion sheaths be at least 18 inches long. An estimate of the required length is given in Appendix C.

2. THERMOELECTRIC PROPERTIES

It is well known that for solid state materials, the thermoelectric figure of merit of semiconductors is much higher than that of metals and insulators; insulators having the least, on account of very high electrical resistivity values. Not too much is known, however, about the figure of merit for liquid state materials. Based upon the quantitative calculations for the thermoelectric figure of merit given in Chapter V, it appears that the metals examined in this investigation may offer more advantages thermoelectrically in the liquid state than in the solid state. This was concluded assuming that the Wiedemann-Franz-Lorenz law were valid for the liquid state also.

If the thermoelectric figures of merit as calculated in Chapter V for liquid metals were correct, liquid semiconductors might have a similar trend. Thus, it might be speculated that liquid semiconductors might be very attractive for the thermoelectric applications. Presently there is no generally accepted theory that can confirm or deny such a speculation. Therefore, it would seem worthwhile to experimentally determine the thermoelectric properties of liquid-state semiconductors too.

REFERENCES

REFERENCES

1. Bidwell, C. C., Phys Rev., 23, 1924, p 357.

2. Bronewski, W., and L. Hackspill, C. R. Acad. Sci., Paris, 153, 1911, p. 814.

3. Heiber, E., Ann. Phys., LpZag, 23 (2), 1935, p. 111.

4. Bradley, C. C., Philosophical Magazine, 7, 1962, p. 1337.

5. Marwaha, A. S., Advances in Physics, 16 (64), Oct. 1967, p. 617.

6. Liquid Metals Handbook, Jackson ed. Washington: Atomic Energy Commission and U.S. Navy, 1952.

7. Cusack, N. E., Rep. Prog. Phys., 26, 1963, p. 361.

8. Angrist, S. W., Direct Energy Conversion, Allyn and Bacon, Inc., Boston, 1965.

9. Jakob, M., Heat Transfer, Vol. I, John Wiley and Sons, New York, 1958.

10. Semat, H., and R. Katz, Physics, Vol. II, Rinehart and Company, Inc., New York, 1960.

11. Wiedemann, G., and R. Franz, "The Thermal Conductivities of Metals," Ann. Physik, 13, 1928, pp. 422-447.

12. Soo, S. L., Direct Energy Conversion, Prentice-Hall, Inc., New Jersey, 1968.

13. Ziman, J. M., Philosophical Magazine, 6, 1961, p. 1013.

14. Phillips, J. C., and L. Kleinman, Phys, Rev., 116, 1959, pp. 287, 880; ibid, 117, 1960, p. 460; ibid, 118, 1960, p. 1153.

15. Bradley, C. C., T. E. Faber, E. G. Wilson, and J. M. Ziman, Philosophical Magazine, 7, 1962, p. 865.

16. Harrison, W. A., Pseudopotentials in the Theory of Metals, W. A. Benjamin, Inc., New York, 1966.

17. Sundstrom, L. J., Philosophical Magazine, 11, 1965, p. 657.

18. Marwaha, A. S., and N. E. Cusack, Physics Letters, 22 (5), North-Holland Publishing Co., Amsterdam, 15. September, 1966.

19. White, R. M., Sandia Laboratory Report SC-RR-68-588, 1968.

20. Landolt-Bornstein, "Physikalisch-chemische Tabellen," 6th ed. Vol. 11/6, Springer, Berlin, 1959, p. 929/31.

APPENDICES

APPENDIX A

LIQUID-METAL TEST APPARATUS DESIGN DETAILS

A list of material and the design details of the liquid metal test apparatus are presented in this appendix.

LIST OF MATERIAL

Piece No.	Quantity	Description
1	1	Upper tantalum part
2	1	Beryllia tube
3	1	Type 304 stainless steel cap
4	1	Lower tantalum part
5	1	Junction tip sheath, copper
6	6	Type 316 stainless steel stud No. 8-32UNC-2A, 1 1/2" long thread length 1/2" each end
7	6	Mullite tube (1/4" OD x 3/16" ID x 5/8" long)
8	1	Removable tantalum plug 3/8 NPT
9	2	Thermocouple manufactured by the Thermo-Electric Company, specifications as follows: tantalum sheath, ceramo type CETA-116K chromel-alumel 6" immersion length, grounded junction with 1/16" NPT adjustable fitting
10	1	Gasket, Garlock
11	1	Back-up ring, copper
12	6	Flat washer, stainless steel
13	12	Nut, No. 8-32UNC-2B, stainless steel
14	6	Lock washer for No. 8 screw, stainless steel

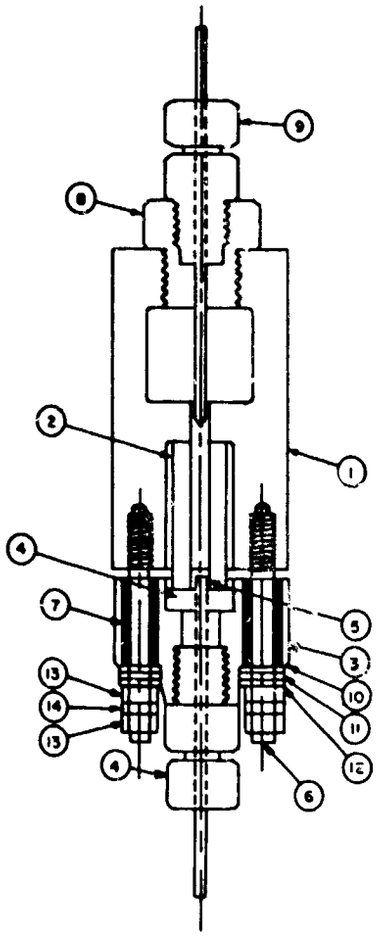

LIQUID METAL

TEST APPARATUS ASSEMBLY

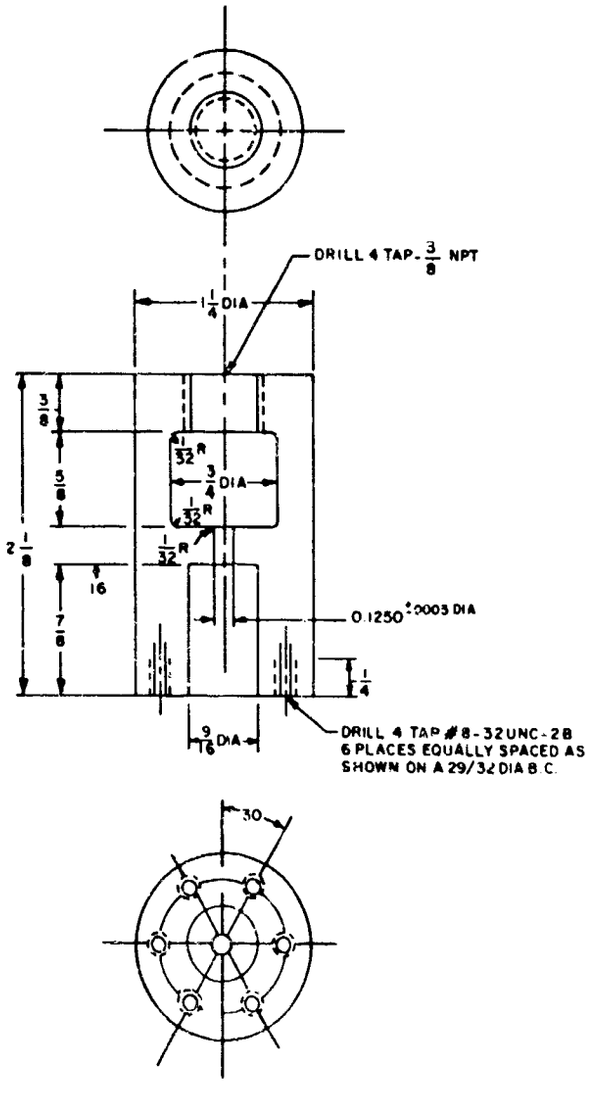

(1) UPPER TAUTALUM PART

FIGURE 12
DESIGN DETAILS

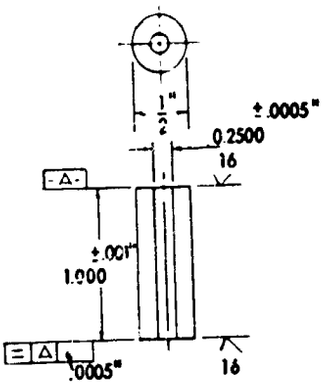

(2) BERYLLIA TUBE

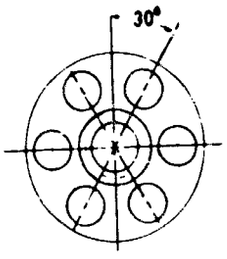

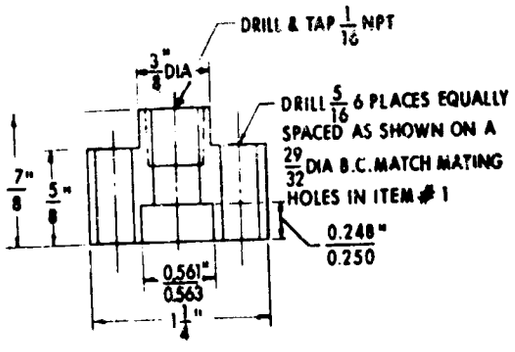

(3) CAP

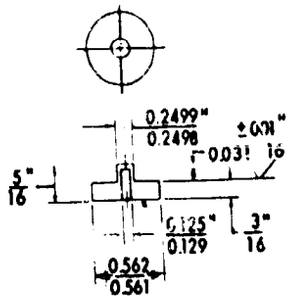

(4) LOWER TAUTALUM PART

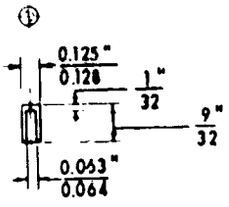

(13) NUT-SQUARE NO. 8-32 UNC-2B MTL SST - (GRIND NUT TO SHAPE SHOWN BY SOLID LINES - 1/4" ACROSS ALL FLATS 12 REQ.)

(5) THERMOCOUPLE JUNCTION TIP SHEATH - MTL CU. - 1 REQ.

FIGURE 12
(CONTINUED)

APPENDIX B

ESTIMATE OF ERROR IN SEEBECK-COEFFICIENT

1. METHOD

The final form of the equation used to calculate the absolute Seebeck coefficient of the metals tested in this investigation is given by

$$S_S = S_{SW} + S_{WPt} + S_{Pt} \quad . \tag{25}$$

The errors, dS_{SW}, dS_{WPt}, and dS_{Pt}, associated with S_{SW}, S_{WPt}, and S_{Pt}, respectively, on the right side of Equation (25) are uncorrelated. That is, S_{SW} was determined experimentally while S_{WPt} and S_{Pt} were obtained from the literature. The total error in S_S may be expressed as

$$dS_S = \left[dS_{SW}^2 + dS_{WPt}^2 + dS_{Pt}^2 \right]^{1/2} \tag{26}$$

Each of the individual errors will now be discussed. Consideration is given first to the error in S_S.

The mathematical expression for S_{SW} is given by

$$S_{SW} = \frac{V_{SW}}{T_H - T_C} \quad , \tag{27}$$

where V_{SW}, T_H, and T_C are experimentally measured quantities and S_{SW} is an explicit function of V_{SW}, T_H, and T_C

$$S_{SW} = f(V_{SW}, T_H, T_C) \quad . \tag{28}$$

Therefore, the error, dS_{SW}, may be found from the total derivative of Equation (28)

$$dS_{SW} = \frac{\partial S_{SW}}{\partial V_{SW}} dV_{SW} + \frac{\partial S_{SW}}{\partial T_H} dT_H + \frac{\partial S_{SW}}{\partial T_C} dT_C , \tag{29}$$

where, from Equation (27),

$$\frac{\partial S_{SW}}{\partial V_{SW}} = \frac{1}{T_H - T_C} \tag{30}$$

$$\frac{\partial S_{SW}}{\partial T_H} = - \frac{V_{SW}}{(T_H - T_C)^2} \tag{31}$$

$$\frac{\partial S_{SW}}{\partial T_C} = + \frac{V_{SW}}{(T_H - T_C)^2} . \tag{32}$$

Substituting Equations (30), (31), and (32) into Equation (29) gives

$$dS_{SW} = \frac{dV_{SW}}{T_H - T_C} - \frac{V_{SW}}{(T_H - T_C)^2} dT_H + \frac{V_{SW}}{(T_H - T_C)^2} dT_C . \tag{33}$$

which can be rewritten in terms of S_{SW},

$$dS_{SW} = \frac{1}{T_H - T_C} \left[dV_{SW} - S_{SW} (dT_H - dT_C) \right] . \tag{34}$$

The error, dS_{SW}, can now be determined from estimates of the errors, dV_{SW}, dT_H, and dT_C, since everything else is known. These estimates are now presented beginning first with dV_{SW}.

2. ERRORS IN MEASURING V_{SW}

The principal errors considered in the measurement of V_{SW} result from instrumentation errors. These errors, based on the manufacturer's specification data for the Vidar 520-01 integrating digital voltmeter, are presented below, in terms of the full-scale (F.S.) value of the digital voltmeter except where noted otherwise.

Source of Error	Amount
Linearity	±.004 per cent F.S.
F.S. Drift	±.01 per cent F.S.
F.S. Temperature Coefficient*	±.015 per cent F.S.
Zero Drift	±.015 per cent F.S.
Zero Temperature Coefficient*	±.03 per cent F.S.
Line Voltage Variation	±.0005 per cent F.S.
Count-Count Variation	±.002 per cent F.S.
Noise	±2.5 μV.

The full scale value used on the digital voltmeter was 10 mV. However, the maximum value of V_{SW} recorded in the experiments was no higher than 2 mV. The lowest value recorded was about 50 μV.

Using a recorded value of 2 mV the errors from each source presented previously should be no higher than the values presented on the next page.

*Assuming ±5°C room temperature variation.

Source of Error	Amount
Linearity	± .08 μV
F.S. Drift	± .2 μV
F.S. Temp. Coef.	± .3 μV
Zero Drift	± .2 μV
Zero Temp. Coef.	± .6 μV
Line Volt. Variation	± .01 μV
Count-Count Variation	± .04 μV
Noise	±2.5 μV

The maximum limits of error are found by adding the values just given. This turns out to be

$$dV_{SW} \leq \pm 3.93\,\mu V . \tag{35}$$

However, it is unlikely that at any given measurement the maximum error would occur. Therefore, the most probable error calculated below using a similar form as Equation (26) gives

$$dV_{SW} \leq \pm \sqrt{.08^2 + .2^2 + .3^2 + 2^2 + .6^2 + .01^2 + .04^2 + 2.5^2}$$

$$dV_{SW} \leq \pm \sqrt{6.7881} \leq \pm 2.60\,\mu V . \tag{36}$$

The per cent error based on the maximum reading is therefore,

$$V_{SW} \leq \pm \frac{2.60\,\mu V}{2000\,\mu V} \times 100 \text{ per cent}$$

$$\leq \pm 0.13 \text{ per cent} . \tag{37}$$

3. ERRORS IN MEASURING T_H AND T_C

Instrumentation error. Following the same procedure used to determine the error in V_S, the instrumentation error for T_H and T_C turns out to be

$$(dT_H = dT_C)\ \underset{\text{max. error}}{\overset{\text{instrumentation}}{\leq}}\ \pm 11.25\,\mu V\ , \tag{38}$$

and, the most probable error turns out to be

$$dT_H = dT_C \leq \pm 4.85\,\mu V\ . \tag{39}$$

The relatively large error results from the use of a larger full scale value of 30 mv with the same percentage errors as given previously for the instrumentation. Also the per cent error in linearity increased from 0.004 per cent to 0.02 per cent because the thermal emf of chromel-alumel thermocouples at high temperatures requires a larger range of the digital voltmeter up to about 25 mV at 600°C.

The instrumentation error, $dT_H = dT_C \leq \pm 11.25\,\mu V$, corresponds to ±.01 mV or a maximum temperature variation of ±0.25°C. The most probable error corresponds roughly to ±0.12°C.

Thermocouple accuracy. The emf's of two thermocouples for use in the test apparatus were checked at the freezing and boiling points of distilled water at a barometric pressure of 29.92 in. Hg.

The thermal emf's measured at the ice point were ±.001 mV corresponding to 0°C in each case. The values recorded at the boiling point averaged +4.080 mV for one thermocouple, while the other thermocouple averaged +4.081 mV.

At 100°C, these results indicated an error of -1/2 per cent or -0.5°C as compared to NBS - table values. Generally chromel-alumel thermocouples are more accurate at higher temperatures. Therefore, it was assumed that an error of about 1/2 per cent would be conservative throughout the entire temperature range from 100°C to 600°C.

Transient response in T_H and T_C measurements. Temperature measurements of the liquid metals in these experiments were made under non-steady state conditions. As the data were taken for the most part while the apparatus was being heated, the thermocouple junction temperatures probably lagged slightly behind the temperature of the liquid metal. However, due to the unknown temperature distribution, the thermocouple junction temperatures may have lead the temperature of the liquid metal.

For the estimation of the maximum temperature difference, it is assumed that the internal resistance of the spherical junction of the thermocouples shown in Figure 2, p.10, can be neglected with respect to the tantalum sheaths and additional layers. A check of a modified Biot-modulus shows that this assumption seems to be justified. Therefore, the maximum temperature difference at the upper junction is approximately

$$T_j - T_L = \pm \frac{dT_j}{d\theta} \frac{\rho_j (Cp)_j D\delta_{Ta}}{4k_{Ta}}$$

$$= \pm \left[\left(300 \frac{°C}{HR}\right) \frac{\left(550 \frac{lbm}{FT^3}\right)\left(0.1 \frac{Btu}{lbm\,°F}\right)(0.04in.)(0.01in.)}{(4)\left(30 \frac{Btu}{HR\,FT\,°F}\right)} \right] = 1.3 \times 10^{-6}\,°C \approx 0°C \qquad (40)$$

and at the lower junction

$$T_j - T_L = \pm \frac{dT_j}{d\theta} \rho_j (Cp)_j V_j \left[\frac{\delta_1}{k_1 A_1} + \frac{\delta_2}{k_2 A_2} + \frac{\delta_3}{k_3 A_3} \right]$$

$$= \pm \left(300 \frac{°C}{HR}\right)\left(550 \frac{lbm}{FT^3}\right)\left(0.1 \frac{Btu}{lbm\,°F}\right)(6 \times 10^{-7}\ FT^3)$$

$$\times \left[\frac{(.01\ in.)\ (12\ in.)}{\left(30 \frac{Btu}{HR\ FT\ °F}\right)(004 in.^2)(1\ FT)} + \frac{(03\ in.)\ (12\ in.)}{\left(200 \frac{Btu}{HR\ FT\ °F}\right)(.01\ in.^2)(1\ FT)} \right.$$

$$\left. + \frac{(03\ in.)\ (12\ in.)}{\left(30 \frac{Btu}{HR\ FT\ °F}\right)(.05\ in.^2)\ (1\ FT)} \right] = 0.0059°C \ . \qquad (41)$$

Therefore it is assumed that the response error in each of the thermocouple junctions can be neglected.

Conduction error in T_H and T_C measurements. Since the thermocouples are made up of materials which have roughly the same thermal conductivity, the conduction error associated with the T_H and T_C measurements can be estimated by assuming a homogeneous rod where heat is conducted along its axis to or away from the liquid metal interface. The temperature difference between the liquid metal interface and the thermocouple junction now can be estimated from the solution for a pin fin with a finite length, where heat losses at the ends are neglected.

$$\frac{T_j - T_\infty}{T_L - T_\infty} = \left[\frac{e^{m\delta}}{1 + e^{2m\ell}} + \frac{e^{-m\delta}}{1 + e^{-2m\ell}} \right] \qquad (42)$$

where

ℓ = length of thermocouple sheath

T_∞ = maximum temperature of argon around the transition tube containing the epoxy

= 100°C

T_L = liquid metal temperature = 600°C

δ = thickness of materials above thermocouple junction. For the upper junction δ = .0008 FT. For the lower junction δ = .0056 FT.

and

$$m = \sqrt{\frac{h4}{kD}} = 7.3/FT \tag{43}$$

where

h = convective heat transfer coefficient, (assumed 2 Btu/hr ft^2 °F)

k = thermal conductivity, (assumed 30 Btu/hr FT °F)

D = diameters of thermocouple junction, (.005 FT)

Substituting above values in Equation (42) leads to a dimensionless temperature difference For the upper junction,

$$\frac{T_j - T_\infty}{T_L - T_\infty} = \left[\frac{e^{(7.3)(.0008)}}{1 + e^{2(7.3)(.5)}} + \frac{e^{-(7.3)(.0008)}}{1 + e^{-2(7.3)(.5)}} \right] = 1. \tag{44}$$

Thus, $T_j \simeq T_L$ and the conduction error will be assumed to be negligible at the upper junction.

For the lower junction, we calculate

$$\frac{T_j - T_\infty}{T_L - T_\infty} = \frac{e^{(7.3)(.0056)}}{1 + e^{2(7.3)(.5)}} + \frac{e^{-(7.3)(.0056)}}{1 + e^{-2(7.3)(.5)}} = .996 \qquad (45)$$

and

$$T_j = .996\,(600 - 25) + 25 = 599°C$$

thus

$$T_L - T_j = 1°C\ .$$

Summary of temperature errors

Error Source	dT_H	dT_C
Instrumentation	±0.12°C	±0.12°C
Response	Negligible	Negligible
Conduction	0.0	±1.0°C at 600°C
Totals	±.12°C	±1.12°C

It is seen that these errors leave a maximum value of

$$dT_H - dT_C = \pm 1.24°C \text{ maximum}\ . \qquad (46)$$

It will be assumed that the total error $dT_H - dT_C$ varies linearly with temperature from 100°C to 600°C. Substituting the estimated errors as found in the preceding discussions into Equation (34) gives a maximum error,

$$dS_{SW} = \frac{1}{T_H - T_C}\left[\pm 2.6\ \mu V - S_{SW}\ (\pm 1.24°C)\right]\ . \qquad (47)$$

However, the maximum most probable error is expected to be

$$dS_{sw} = \pm \frac{1}{T_H - T_C} \left[2.6^2 + (1.24\, S_{SW})^2 \right]^{1/2} \tag{48}$$

$$dS_{SW} = \pm \frac{1}{T_H - T_C} \sqrt{6.76 + 1.54\, S_{SW}^2}\,. \tag{49}$$

With the results of Equation (49) the errors in S_{SW} for each of the metal samples are estimated as follows:

Sodium Error Calculation

	(1) Low Temperature Data	(2) High Temperature Data
$\bar{T}$	220°C	605°C
ΔT	11°C	11°C
S_{NaCh}	-36 μV/°C	-33 μV/°C
S_{NaAl}	+7.55 μV/°C	+10 μV/°C

(1) $$dS_{NaCh} = \pm \frac{1}{11} \sqrt{6.76 + (.23)(36)^2} = \pm 1.58\ \mu V/°C \tag{50}$$

(1) $$dS_{NaAl} = \pm \frac{1}{11} \sqrt{6.76 + (.23)(7.55)^2} = \pm .40\ \mu V/°C \tag{51}$$

(2) $$dS_{NaCh} = \pm \frac{1}{11} \sqrt{6.76 + (1.54)(33)^2} = \pm 3.6\ \mu V/°C \tag{52}$$

(2) $$dS_{NaAl} = \pm \frac{1}{11} \sqrt{6.76 + (1.54)(10)^2} = \pm 1.15\ \mu V/°C\,. \tag{53}$$

Potassium Error Calculations

	(1) Low Temperature Data	(2) High Temperature Data
$\bar{T}$	315°C	586°C
ΔT	7.75°C	31°C
S_{KCh}	-45.81 μV/°C	-50.37 μV/°C
S_{KAl}	-5.55 μV/°C	-7.82 μV/°C

(1) $$dS_{KCh} = \pm \frac{1}{7.55} \sqrt{6.76 + (.45)(45.81)^2} = \pm 4.07\ \mu V/°C \quad (54)$$

(1) $$dS_{KAl} = \pm \frac{1}{7.55} \sqrt{6.76 + (.45)(5.55)^2} = \pm .60\ \mu V/°C \quad (55)$$

(2) $$dS_{KCh} = \pm \frac{1}{31} \sqrt{6.76 + (1.54)(50.37)^2} = \pm 2.03\ \mu V/°C \quad (56)$$

(2) $$dS_{KAl} = \pm \frac{1}{31} \sqrt{6.76 + (1.54)(7.82)^2} = \pm .30\ \mu V/°C. \quad (57)$$

Mercury Error Calculations

	(1) Low Temperature Data	(2) High Temperature Data
$\bar{T}$	92°C	200°C
ΔT	3.25°C	12°C
S_{HgCh}	-26.2 μV/°C	-24.9 μV/°C
S_{HgAl}	+17.5 μV/°C	+15.2 μV/°C

(1) $$dS_{HgCh} = \pm \frac{1}{3.25} \sqrt{6.76 + .06(26.2)^2} = \pm 2.13\ \mu V/°C \quad (58)$$

$$(1) \qquad dS_{HgAl} = \pm \frac{1}{3.25} \sqrt{6.76 + .06(17.5)^2} = \pm 1.54\ \mu V/°C \qquad (59)$$

$$(2) \qquad dS_{HgCh} = \pm \frac{1}{12} \sqrt{6.76 + .19(24.9)^2} = \pm 0.94\ \mu V/°C \qquad (60)$$

$$(2) \qquad dS_{HgAl} = \pm \frac{1}{12} \sqrt{6.76 + 19(15.2)^2} = \pm 0.60\ \mu V/°C\ . \qquad (61)$$

From the foregoing error estimates it can be concluded that the measured Seebeck-coefficients should be accurate to within

±1 per cent for Sodium

±9 per cent for Potassium

±9 per cent for Mercury.

Total error. Values S_{WPt} for chromel and alumel and S_{Pt} are reported in the literature within $\pm 0.1\ \mu V/°C$ each. Based on these deviations the maximum most probable error for the absolute Seebeck coefficient of sodium can be estimated from Equation (26) to be

$$dS_{Na} = \pm \sqrt{dS_{NaW}^2 + dS_{WPt}^2 + dS_{Pt}^2} \qquad (62)$$

$$dS_{Na} = \pm \sqrt{3.62^2 + .1^2 + .1^2} = \pm 3.6\ \mu V/°C\ . \qquad (63)$$

Similarly, we have for potassium and mercury

$$dS_{K} = \pm \sqrt{4.07^2 + .1^2 + .1^2} = \pm 4.1\ \mu V/°C \qquad (64)$$

$$dS_{Hg} = \pm \sqrt{2.13^2 + .1^2 + .1^2} = \pm 2.1\ \mu V/°C\ . \qquad (65)$$

APPENDIX C

ESTIMATE OF RECOMMENDED LENGTH OF THERMOCOUPLE IMMERSION SHEATHS FOR TEST APPARATUS

For an estimate of the recommended length of the thermocouple immersion sheaths it is assumed that the materials making up the thermocouple assembly shown in Figure 2, p. 10, have roughly the same thermal conductivity. For this purpose the following equation is applied

$$T_E - T_\infty = (T_R - T_\infty)\, e^{-mx} \tag{66}$$

where

T_R = the temperature of the thermocouple tube where it leaves the ceramic container, (assumed $\leqq$ 800°C)

T_∞ = room temperature, (assumed = 25°C)

T_E = melting point of epoxy in transition tube, (assumed = 100°C)

and m becomes

$$m = \sqrt{\frac{4h}{kD}} = 7.3/FT \,. \tag{67}$$

For

h = convective heat transfer coefficient, (assumed 2 Btu/HR FT^2 °F)

k = thermal conductivity, assumed (30 Btu/HR FT °F)

D = diameter of thermocouple junction (.005 FT) .

Substituting in Equation (66), we get

$$e^{-7.3x} = \frac{75}{775} = 0.097 \tag{68}$$

and x has to be larger than or equal to .32 ft or about 4 in. Since the ceramic container is 24 in. long and the apparatus is located in the center with the thermocouple junctions about 1 in. apart, the total length of the total thermocouple immersion tubes should be at least 16 in. long.

APPENDIX D

LIST OF SYMBOLS

A	Cross-sectional area of liquid metal sample, (in^2)
A_1	One-dimensional heat conduction area of thermocouple junction, (in^2)
A_2	One-dimensional heat conduction area of copper tip sheath, (in^2)
A_3	One-dimensional heat conduction area of lower tantalum part, (in^2)
C_p	Specific heat, (Btu/lbm ° F)
D	Diameter of thermocouple junction, (in)
E	Applied voltage, (volt)
I	Electric current, (amp)
K	Boltzmann's Constant, (1.38049×10^{-23} Joule/° C)
L	Length between thermocouple probes, (in)
L_o	Lorenz Constant, (2.45×10^{-8} watt-ohm/° K)
R	Electrical resistance of shunt resistor, (ohm)
R_s	Electrical resistance of liquid metal sample, (ohm)
S_{sw}	Relative Seebeck coefficient between sample, (S) and counter electrode (W), (μV/° C).
S_s	Absolute Seebeck coefficient of sample (S), (μV/° C)

S_W	Absolute Seebeck coefficient of material (W), ($\mu V/°C$)
T_C	Temperature of cold side of sample, (° C)
T_H	Temperature of hot side of sample, (° C)
$\bar{T}$	Arithmetic mean temperature of sample, (° C)
T_O	Temperature of reference junction, (° C)
T	Absolute temperature, (° K)
T_L	Temperature of liquid sample (° C)
T_j	Temperature of thermocouple junction (° C)
T_E, T_R	Temperature, explained where used (° C)
V_{SW}	Relative Seebeck voltage between sample (S) and counter electrode (W) (volt).
V_C	Combined voltages due to Seebeck voltage, V_{SW} and IR_S sample voltage (volts).
V_j	Volume of thermocouple junction (ft^3)
Z	Thermoelectric figure of merit (1/° K)
a, b, c, d, e, f, g, h, o, c	Symbols in illustrations explained where used
d	Differential
h	Convective heat transfer coefficient (Btu/hr ft^2 ° F)
k	Thermal conductivity of material (Btu/hr ft ° F)

k_1	Thermal conductivity of thermocouple junction (Btu/hr ft ° F)
k_2	Thermal conductivity of copper tip sheath (Btu/hr ft ° F)
k_3	Thermal conductivity of lower tantalum part (Btu/hr ft ° F)
ℓ	Length of thermocouple sheath, (ft)
m	Mass, (grams)
m	Grouping of heat transfer properties and dimensions explained where used.
n	Number density (in^{-3})
q	Electronic charge
Δ	Difference
Π	Peltier coefficient, (μV)
γ	Thomson coefficient, (μV/° C)
δ	Heat transfer dimension (ft)
δ_1	Thickness of lower tantalum thermocouple sheath (ft)
δ_2	Thickness of copper tip sheath (ft)
δ_3	Thickness of lower tantalum part (ft)
δ_{Ta}	Thickness of tantalum thermocouple sheath
δ	Thickness of material between liquid metal interface and thermocouple junction (ft)
ϵ_o	Fermi energy at absolute zero, (joule)
θ	Time (hr)

ρ	Density (lbm/ft^3)
σ	Electrical conductivity, (mho/cm)
τ	Relaxation time (sec)

SUBSCRIPTS

Al	Alumel
C	Cold side
Ch	Chromel
H	Hot side
Hg	Mercury
j	Junction
K	Potassium
L	Liquid
Na	Sodium
O	Reference
Pt	Platinum
S	Sample
Ta	Tantalum
W	Counter-electrode
1, 2, 3	Explained under symbols

SUPERSCRIPTS

—	Average value

UNCLASSIFIED
Security Classification

DOCUMENT CONTROL DATA - R & D

(Security classification of title, body of abstract and indexing annotation must be entered when the overall report is classified)

1. ORIGINATING ACTIVITY (Corporate author) Naval Ship Research & Development Laboratory Annapolis, Maryland 21402	2a. REPORT SECURITY CLASSIFICATION Unclassified 2b. GROUP

3. REPORT TITLE
Investigation of Thermoelectric Properties of Liquid Metals

4. DESCRIPTIVE NOTES (Type of report and inclusive dates)
Research and Development Report

5. AUTHOR(S) (First name, middle initial, last name)
Hugh Grant Anderson, Jr.

6. REPORT DATE November 1969	7a. TOTAL NO. OF PAGES 68	7b. NO. OF REFS 20
8a. CONTRACT OR GRANT NO. NASA Grant 43-001-021 b. PROJECT NO. Sub Account 141370-3514R c. d.	9a. ORIGINATOR'S REPORT NUMBER(S) 3058 9b. OTHER REPORT NO(S) (Any other numbers that may be assigned this report) MACHLAB 254	

10. DISTRIBUTION STATEMENT This document has been approved for public release and sale; its distribution is unlimited.

11. SUPPLEMENTARY NOTES	12. SPONSORING MILITARY ACTIVITY NAVSHIPRANDLAB Annapolis

13. ABSTRACT

An apparatus has been designed and developed for measuring Seebeck potentials and electric resistivities of corrosive liquids up to temperatures of about 600°C. A complete description of the test apparatus and the procedures used in its initial operation up to 600°C are given. Experimental results for the absolute Seebeck coefficients of sodium and potassium are in good agreement with published values from previous investigations performed at temperatures up to 400°C. The obtained values are in the range of 0-40 uV/°C, potassium having the highest values. These results indicate that the absolute Seebeck coefficients in the liquid state seem to be higher than that of the solid state by as much as a factor of about three for both metals. Quantitative calculations indicate that these particular metals offer more advantages thermoelectrically in the liquid state than in the solid state. Results for the electrical resistivity were too high by about four orders of magnitude and therefore they were considered to be erroneous. It is proposed how to improve the test apparatus to obtain more meaningful resistivity values and how to extend the temperature range of the facility to the design temperature 800°C. It is suggested that the thermoelectric properties of liquid semiconductors be investigated in the future. (author)

DD FORM 1 NOV 1473 (PAGE 1)
S/N 0101-807-6801

UNCLASSIFIED
Security Classification

UNCLASSIFIED
Security Classification

14 KEY WORDS	LINK A		LINK B		LINK C	
	ROLE	WT	ROLE	WT	ROLE	WT
experiments						
melting						
furnace						
metals						
liquid metals						
Seebeck coefficient						
resistivity						
instrumentation						
sodium						
potassium						
mercury						
apparatus						

DD FORM 1 NOV 1473 (BACK)
(PAGE 2)

UNCLASSIFIED
Security Classification